Geometry optimization of unidirectional integrated ring laser

PROCEEDINGS OF SPIE

SPIEDigitalLibrary.org/conference-proceedings-of-spie

Geometry optimization of unidirectional integrated ring laser

Giannuzzi, Giuseppe, Ghillino, Enrico, Bardella, Paolo

Giuseppe Giannuzzi, Enrico Ghillino, Paolo Bardella, "Geometry optimization of unidirectional integrated ring laser," Proc. SPIE 11283, Integrated Optics: Devices, Materials, and Technologies XXIV, 112832H (25 February 2020); doi: 10.1117/12.2546419

SPIE.

Event: SPIE OPTO, 2020, San Francisco, California, United States

Geometry optimization of unidirectional integrated ring laser

Giuseppe Giannuzzi[a], Enrico Ghillino[b], Paolo Bardella*[a]
[a]DET, Politecnico di Torino, Corso Duca degli Abruzzi 24, 10129 Torino, Italy
[b]Synopsys, Inc., 400 Executive Blvd Ste 101, Ossining, NY 10562, United States

ABSTRACT

Ring lasers, evanescently coupled to an adjacent optical waveguide, are essential components for the upcoming generation of integrated sources. In an ideally symmetric resonator, emission occurs from the both clockwise and counter-clockwise directions, resulting in a potential waste of emitted optical power, while unidirectional emission has been reported in different configurations, for example when asymmetric external reflectivities are used for the coupling waveguide. In the integrated form, a common approach consists in the inserting an S-bend waveguide in the ring, in such a way that the field propagating in the direction that we want to suppress is reinjected in the other direction. The S-bend waveguide must be carefully designed to reduce optical losses and to ensure a sufficient suppression of the undesired field. Using 2D finite-difference time-domain simulations performed with Synopsys RSoft©, we report a systematic analysis of the racetrack geometry of a 86.8 μm long microring laser including an inner S-waveguide, and we maximize the unidirectionality of the ring laser, scanning the gap distance between external racetrack resonator and S-bend waveguide. The results of this numerical analysis can be finally used to generate the mask layout of the improved unidirectional ring laser, targeting a Process Design Kit of choice, taking advance of the integration of RSoft with the software OptoDesigner©.

Keywords: ring resonator, semiconductor ring lasers, photonic integrated circuits, finite-difference time-domain, unidirectional ring lasers, numerical analysis, laser resonators, RSoft software.

1. INTRODUCTION

Lasers based on microcavities are attractive for their compactness, low threshold, low power consumption, and potential for ultrafast modulation speed. In particular, the microsized semiconductor ring lasers (SRLs) have the advantage to be embedded into the photonics integrated circuits (PICs). The laser power from the ring cavity is transferred to other fundamental elements in PICs, for instance by means of a waveguide close to the ring, namely a directional coupler.

SRL is a bidirectional laser, which cavity supports two beams corresponding to the clockwise (CW) circulating direction and the counterclockwise (CCW) ones. Nevertheless, unidirectional SRL is desirable in optical interconnects. The reasons for this are an improved longitudinal mode purity and an enhanced output power in the pre-arranged direction of propagation as well as a less sensitivity to the back-reflections. Moreover the unidirectionality ensures a more linear light-vs-current (L-I), eliminating kinks due to the competition between the two counterpropagating lasing modes[1]. The unidirectionality in an SRL can be reached through unbalanced loss mechanism or vice versa nonreciprocal gain for the two propagation directions inside the ring.

Some works report spontaneous unidirectional lasing in case of triangular SRLs[2,3] and large diameter SRLs[4], when bistable unidirectionality could arise. The sidewall roughness of the waveguide or some imperfections along the ring could give rise to such unidirectional bistability, where only one between CW or CCW lasing directions becomes dominant while the other is strongly suppressed, but in principle the lasing direction is unpredictable.

In other works, different approaches were proposed to force unidirectional operation in SRLs. Hohimer et al.[1,5] reported for the first time the unidirectional operation in a semiconductor ring diode laser, thanks to the use of an active crossover waveguide which benefitted unidirectional lasing in clockwise ring direction. The S-section waveguide linked with Y splitters to the ring, redirects part of the wave-packets propagating in the CCW direction into the opposite CW direction. The same approach was also used by Cao et al.[6] in a semiconductor ring laser with quantum-dot active region.

*paolo.bardella@polito.it; phone +39 0110904208

Integrated Optics: Devices, Materials, and Technologies XXIV, edited by Sonia M. García-Blanco, Pavel Cheben, Proc. of SPIE Vol. 11283, 112832H · © 2020 SPIE
CCC code: 0277-786X/20/$21 · doi: 10.1117/12.2546419

In order to break off the natural symmetrical behavior of the SRLs, Liang et al.[7] simple altered the waveguide shape, including a tapered waveguide inside the triangular ring laser cavity.

Other authors[8–10] forced the lasing output emission from the preferred ring direction, operating outside the ring by means of a feedback mechanism from a cleaved end-facet mirror. The latter reflects back the beam into the laser cavity, so that the ring output in the CCW (or CV) direction after reflection is re-coupled in the ring into the CW (or CCW) direction. In particular, Cai et al.[8] studied as changing the angle between the sidewall of the mirror facet and the plane of ring impacted adversely upon the feedback strength.

The Whistle-geometry semiconductor laser (WRL)[11] is another example of how to induce asymmetry between counterpropagating modes, hence promoting unidirectionality.

Major progresses have recently been obtained introducing a S-bend waveguide inside the ring which evanescently couples the resonator field in correspondence of two couplers[12,13]. Hayenga et al.[13] used this design with the aim to enhance the emission of radiation in a direction perpendicular to the chip growth plane, enforcing the unidirectional operation in an active microring. Similar to the S-crossover waveguide of Hohimer[1], the S-bend waveguide allows the mode conversion from CCW mode to CW (or vice versa if the S is flipped) together to relating nonreciprocal outcoupling loss. Only a fraction of the coupled power in the S-waveguide is truly commuted in the opposite mode. The main difference between the two S-waveguide strategy, with the "S" waveguide linked or not with the resonator, is proper based on the intrinsic losses of the designed device.

In this work, the SLR under investigation was a racetrack with an S-bend waveguide which evanescently couples the field by means of two coupling regions. Such a structure was analyzed using the Finite Difference Time Domain method available in the RSoft simulation software, varying the design parameters, namely the gap between the racetrack and the S-waveguide, in order to optimize the unidirectional lasing.

Moreover, this work focusses only on the design of the SRL that favoring the unidirectional operation, without considering the nature of the active region. For this reason, the simulated device structure consists just on Si waveguides on $Si0_2$, while the simulations of active devices will be the focus of future works.

2. PROPAGATION IN A SLR WITH A S-WAVEGUIDE

Figure 1 reports the schematic of two slightly different SRLs which include a S-shaped waveguide. As already mentioned, the purpose of the S-waveguide is to promote the resonant cavity unidirectionality, promoting the clockwise direction for the design of Figure 1. To highlight this behavior, let us consider two counterpropagating modes circulating in the cavity, describing the optical events that they encounter along a full revolution of the resonator. Let us consider to fix the launch position for both the modes on the right side of the design (A) as reported in Figure 1, looking at only the propagation of the fundamental mode TE of the waveguide.

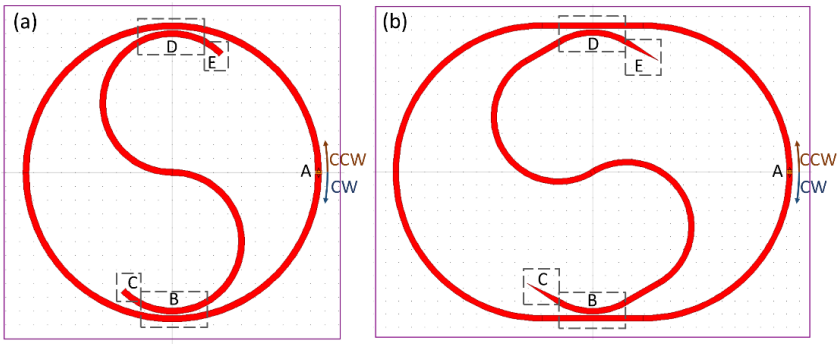

Figure 1 Schematic of SRLs with a S-waveguide inside. In (a), a simple schematic of a ring resonator and a S-waveguide made of two semi-circumferences is shown. In (b), the SRL consists of a racetrack and a S-shaped waveguide of more complex geometry, which includes tapered terminators. CW and CCW represents the two counterpropagating modes, excited from position A. Areas B and D indicate the coupling regions while C and E are the S-waveguide terminators.

First of all, let us examine the field propagating in the CW direction across the device of Figure 1a. The field excited in A propagates in a quarter of circumference without significant modification before meeting the first optical event, i.e. the coupling between the waveguide of the ring and the S-arc portion (B). According to the geometry of the coupling region, part of the radiation leaves the ring, ending in the blind branch of the S-waveguide (C) while the remaining part propagates along the resonator. Two comments can be made. The CW field coupled with the S-waveguide would be the smallest possible, because the CW direction is the one promoted in our design. Moreover, the coupled energy in the S must not be back reflected otherwise it is converted in the undesirable CCW mode. Then, the CW mode propagates in the left-side of the ring and then meets the coupler (D) in the top of Figure 1a, analogue to the previous one. Finally, the part of field that continues to propagate along the ring waveguide reaches the starting point (A) completing the round.

Let's now discuss about the CCW field emerging from the launch position (A). It undergoes a breakdown in the coupling region between the two close waveguides (D). The fraction of field which goes ahead in the ring will be again partitioned in the followed coupler (B). The CCW field comes back to the launch position attenuated while the evanescently coupled field that goes through the S-waveguide is driven within it until the subsequent coupler in the opposite side of S (from D to B, or vice versa). The coupling region leads part of the field into the ring, which propagates in the CW direction, while the remaining field propagates toward the end of the S (C or E). There, it is desirable to minimize back reflections not to feed the CCW mode. Moreover, the CCW field should have a significant coupling with the S-waveguide for both the couplers in order to maximize its conversion in the right direction.

In summary, whilst the CW field results attenuated during the roundtrip, the CCW not only softens but a portion of it is converted in the opposite field thanks to the S-waveguide. The round-trip losses experienced by the CCW field are therefore much higher than the corresponding losses of the CW field; the lasing threshold of the latter is then lower.

In this discussion, the bending losses have not been considered. Nevertheless, they contribute equally to both modes along the external ring.

The simple geometry of Figure 1a, consisting in an external perfectly circular ring, was replaced by the racetrack of Figure 1b, which was used in this work for a more systematic study, varying the gap distance between the racetrack and the S-waveguide while keeping fixed the racetrack length. Regarding the S-waveguide design, it let to vary its length without changing or moving the coupling regions (B and D). On the other hand, to avoid back reflection in correspondence of the extremities of the S-waveguide (C and E), the design includes tapered ends, which rather spread outside the waveguide the field (radiation loss). The reflected field were considered negligible. To reduce the simulation time cost and the footprint in real chips, the device of Figure 1b must have the smallest geometrical area. The minimum radius of the bent waveguide was fixed at 5 μm because nowadays this value guarantees negligible curvature losses for most Silicon Photonics platforms. In the simplest case of Figure 1a, with a waveguide width of 0.45 μm, the minimum geometrical ring path is equal to $2\pi R = 2\pi(10.45\ \mu\text{m} + gap)$, where gap is the distance between the ring and the S waveguides. Considering the racetrack path length of Figure 1b slightly above to the ring ones (Figure 1a), the design allowed more flexibility during simulations in term of racetrack length itself, S-waveguide length and relative gap distance between them.

3. RESULTS AND DISCUSSION

The designed device of Figure 1b was simulated in RSoft software using FullWAVE module which implements a Finite-Difference Time-Domain (FDTD) method. The silicon rib waveguides were operating around 1550 nm, while the substrate was silicon oxide. Spectral dispersion of optical properties was included. In order to reduce the computational cost of the simulations, the 3D domain was reduced using the effective refractive index method (2.5D).

The silicon optical waveguides (both racetrack and channels) were 0.45 μm wide and 0.22 μm high, allowing for the propagation of the fundamental TE mode. The ring length was fixed to 86.8 μm while the S-waveguide was half-cavity long, measured between the two directional couplers. The radius of curvature in the S-waveguide was 5 μm.

To highlight the conversion between the counter-propagating modes due introducing the S-waveguide inside the racetrack resonator, the only racetrack of same geometry was itself simulated in RSoft. In a single run, RSoft allows to introduce 32 electromagnetic sources simultaneously. In this work the position of the sources was randomly selected along the racetrack cavity. From 16 random positions along the racetrack two pulses were radiated, one propagating in the CW direction and the other in the CCW one. Pulsed sources were selected as launch mode in RSoft because they allow to investigate the dispersion behavior of propagation at different wavelengths. The pulse was centered at 1.55 μm.

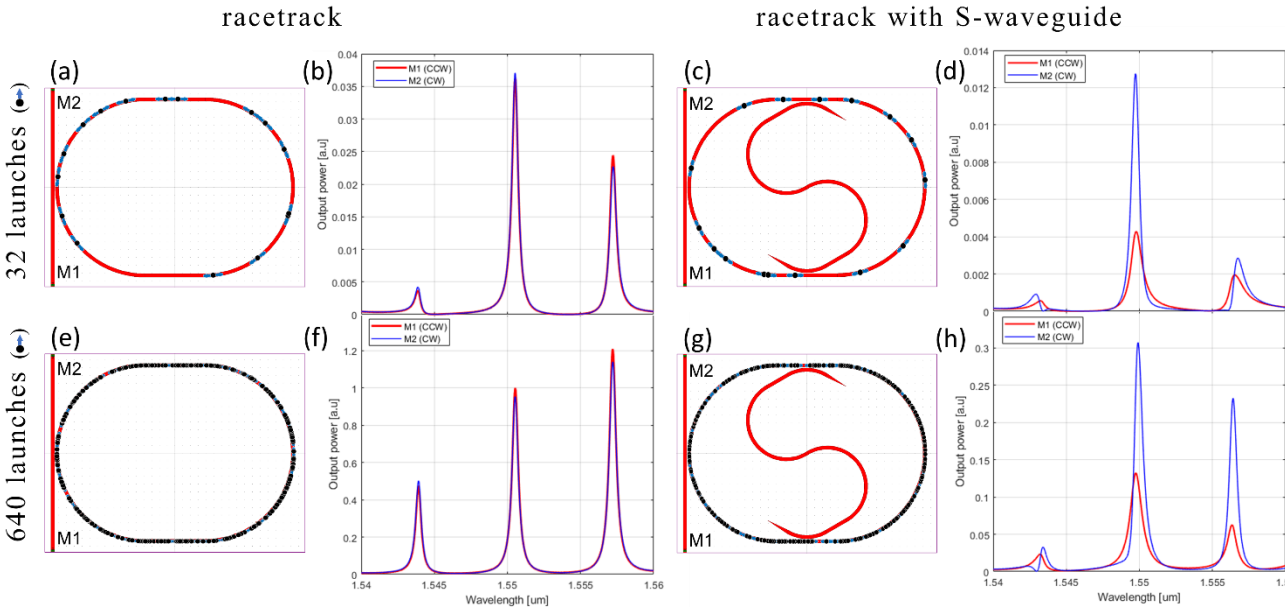

Figure 2 Design and simulation on RSoft software of the racetrack resonator long 86.8 µm in the symmetric and asymmetric configuration. (a) The layout with only the racetrack shows an examples distribution of 16 launch positions (black dots) for both CW and CCW sources. (b) Emission spectra of (a) associated with CCW and CW mode, from monitor M1 and M2 respectively. (c) Racetrack resonator with the S-waveguide and a gap between them of 0.10 µm. (d) Emission spectra induced by the launches distribution of (c). (e) and (g) show the same design of (a) and (c) with the overall distribution of the 640 launches. (f) and (h) report the overall CW and CCW optical spectra of (e) and (g) design, respectively.

Figure 2a and Figure 2c show an example of launch distribution in the case of the only racetrack and with the S-waveguide, respectively. The simulated racetrack designs differ from that of Figure 1b for the presence of the waveguide on the left, where the resonator field in the racetrack is coupled and hence measured in correspondence of two monitors placed at the top and bottom of the waveguide itself, respectively, were the field is saved. The Monitor 1 (M1 in Figure 2) is placed at the bottom and it returns the electrical field emerging from the resonator circulated in CCW direction. Vice versa, the Monitor 2 (M2 in Figure 2) is placed at the top, and it tracks the field emerging from the racetrack CW circulated. For the sake of simplicity, in the following, the two monitors will be referred to as CW monitor and CCW monitor. The gap distance between the lateral waveguide and the racetrack was set to 100 nm for all the simulations.

From the oncoming fields at the monitors, the RSoft simulation returns the wavelengths spectra emerging from the specific simulated structure, hence Figure 2b from Figure 2a and Figure 2d from Figure 2c, in a wavelength interval of 20 nm centered at 1550 nm.

As expected in the case of the ring resonator, the optical spectra of the Figure 2b-Figure 2d show peaks in correspondence of the resonant wavelengths. The resonance peak of interest in this work corresponds to that around 1550 nm. Comparing the two simulated spectra, an unbalance between the two counter-propagating modes was observed in Figure 2d awing purely to the S-waveguide. To quantify such unbalance, a directional extinction ratio (DER)[14,15] was introduced, defined as the ratio, expressed in decibels, of the total output CW power to the CCW power captured by the two monitors previously described:

$$\mathrm{DER} = 10\log_{10}\left|\frac{E_{CW}}{E_{CCW}}\right|^2 = 10\log_{10}\left|\frac{E_{M2}}{E_{M1}}\right|^2. \quad (1)$$

The higher the DER value is, the greater the unidirectionality of the device.

From the simulations shown in Figure 2b,d, DER = 0.078 dB and DER = 4.779 dB, respectively. For the symmetrical configuration with the alone racetrack, whereas ideally DER = 0 dB, a non-zero value of this indicator highlights the strong dependence of the measured field intensity from the positions of the sources. The same comment on the influence of the initial launch position holds for the asymmetrical configuration with the S-waveguide.

For this reason, in order to improve the accuracy of the results, we repeated the simulations 20 times, for different initial launch positions, randomly chosen, keeping fixed the monitors locations. The single simulations results are not shown for sake of brevity. Regarding the racetrack with the S-waveguide, the average value of the unidirectionality factor is DER =3.157 ± 2.760 dB. On the other hand, the racetrack returns DER = 0.059 ± 0.261 dB with no clear predominance between CW and CCW fields. The final unbalanced effect of the S-waveguide has been proved with a predominance of the CW field propagation.

The simulations with the S-waveguide furthermore reveal that the outgoing power from the monitors results always smaller than that with the simple racetrack. This is because the fraction of propagating field in the ends of the S-waveguide was lost. In this regard, the pointed geometry of the S-extremities avoids the back reflections, while the power is spread over a large spatial angle outside the waveguide.

Figure 2e-h show a different analysis of the simulation results for both the above discussed configurations, with/without the S-waveguide. The fields of the 20 simulations for each structure are summed and the final result returns the overall optical spectrum of the 640 launches randomly located along the resonator path. For the device with single racetrack, Figure 2e summarizes the 320 launches positions together with the two opposite directions of field emission for each of them. Figure 2f shows the evaluated overall spectra. Vice versa, when the S-waveguide is taken into account, the particular spatial distribution of the 640 launches depicted on the racetrack of Figure 2g returns the global spectra of Figure 2h.

Apart the peaks intensity between the spectra of the direct simulations and that of the overall ones, both the analysis return similar considerations. The overall unidirectionality factor is DER = -0.198 dB for the racetrack and DER = 4.035 dB for the unbalanced device, values consistent with the average DER values previously estimated.

In the subsequent simulations the influence of the gap distance between the S-waveguide and the racetrack was investigated. This analysis is justified by the fact that the gap determines the coupling of radiation into the S-waveguide, hence the fraction of radiation that will propagate in the opposite direction in the racetrack. Moreover, the purpose of this analysis was to seek for the gap value maximizing the DER.

According the gap distance, the shape of the racetrack was slightly varied in order to keep fix the physical optical length of the racetrack and the geometry of the S-waveguide. Anyway, as proved by further simulations, such slight variation of the radius of curvature of the racetrack have not influence on the optical spectra and its resonance peaks.

Figure 3 shows the unidirectionality factor in correspondence of the resonant peak around 1.55 μm as a function of the gap racetrack – S-waveguide for fixed gap lateral waveguide – racetrack of 100 nm. As discussed above, for each gap distance were carried out 20 simulations with different launch positions and were evaluated both the average and the overall unidirectionality factor. The latter was shown in Figure 3 in red, while the average U value and its standard deviation was depicted by black circle with error bar. Moreover, the results of the only racetrack, evaluated in the first part of this work, were reported as reference values in blue, in the right part of Figure 3.

As shown by Figure 3, the S-waveguide promotes the predominance of the CW field with respect to the CCW ones and such effect results as strong as the gap distance was reduced. Vice versa, with large gap, already since 250 nm, the effect of the S-waveguide becomes obviously negligible and the average value of the unidirectionality factor stood around 0 dB.

It follows that by introducing the S-waveguide and varying the gap, would be possible to modify the ratio between CW and CCW power, hence the DER value.

Our results were obtained from merely geometrical considerations on the racetrack including the S-waveguide, ignoring the active properties of the material. In other works, the device simulated in this work is a passive ring resonator. Nevertheless, the large unidirectionality factor DER (statistically up to 10 dB) reached with small gap racetrack – S-waveguide is expected to be enhanced operating in an active SRL, as supported by the literature[4,14].

Finally, to increase the device unidirectionality, the light coupled inside an active S-waveguide can be further amplified and then injected back into the SRL in the preferred direction, as proved by Sacher et al.[16].This approach could add an unbalanced gain in favor of the CW mode. Nevertheless, such injection operation is subject to the phase and mode matching conditions[1].

The conduced numerical analysis can be used to generate a mask layout of the improved unidirectional ring laser by exploiting the integration of RSoft with the mask layout software OptoDesigner[17].

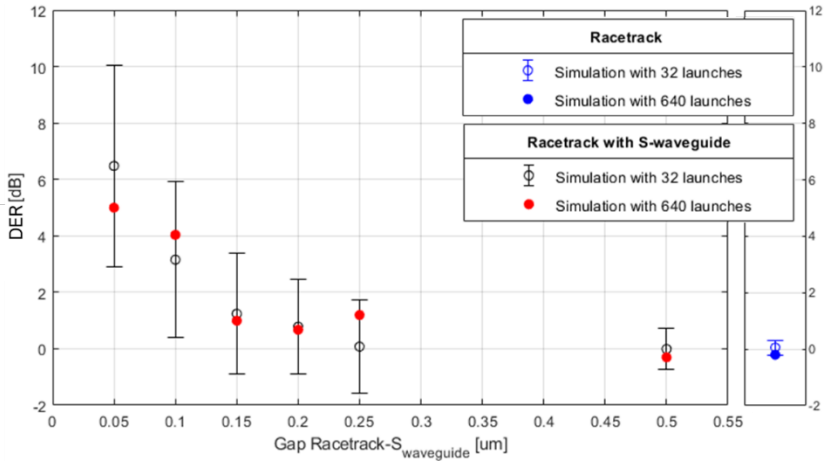

Figure 3 The directional extinction ratio (DER) versus the gap distance between the racetrack and the S-waveguide measured to the peak resonator wavelength around 1550 nm. The result of the 20 simulations for each gap was plotted as average DER value and std in black and as overall DER on the 640 launches in red. On the right, in blue, the reference values for the simulations with only the racetrack.

4. CONCLUSIONS

The SRLs are mainly based on symmetric cavity which supports two beams propagating clockwise and counterclockwise. In this work, numerical simulations were carried out on the symmetric layout of the racetrack resonator equipped with an asymmetric S-shaped internal waveguide. The simulations results were compared with the ones of analogue structures without internal waveguide showing the benefit induced by this additional element in term of the unidirectionality of the SRL. All the simulations were carried out with the FullWAVE module incorporated within RSoft software. Further simulations, varying the gap distance between the resonator and the S-waveguide, evinced that the optimization of unidirectional ring laser can be obtained for gap distance less than 100 nm for the geometrical layout. Moreover, the simulations reveal that the results were extremely affected by the position of the optical sources within the resonator structure and Monte Carlo simulations were needed to properly describe the designed device.

ACKNOWLEDGEMENTS

We would like to thank Andrea Palmieri, Politecnico di Torino, for the fruitful discussions on the use of RSoft software.

REFERENCES

[1] Hohimer, J. P., Vawter, G. A. and Craft, D. C., “Unidirectional operation in a semiconductor ring diode laser,” Appl. Phys. Lett. 62(11), 1185–1187 (1993).
[2] Booth, M. F., Schremer, A. and Ballantyne, J. M., “Spatial beam switching and bistability in a diode ring laser,” Appl. Phys. Lett. 76(9), 1095–1097 (2000).
[3] Ji, C., Booth, M. F. and Ballantyne, J. M., “Low noise operation of a unidirectional triangular ring laser,” Conf. Proc. - Lasers Electro-Optics Soc. Annu. Meet. 2005, 945–946 (2005).
[4] Sorel, M., Laybourn, P. J. R., Giuliani, G. and Donati, S., “Unidirectional bistability in semiconductor waveguide ring lasers,” Appl. Phys. Lett. 80(17), 3051–3053 (2002).
[5] Hohimer, J. P. and Vawter, G. A., “Unidirectional semiconductor ring lasers with racetrack cavities,” Appl. Phys. Lett. 63(18), 2457–2459 (1993).
[6] Cao, H., Deng, H., Ling, H., Liu, C., Smagley, V. A., Caldwell, R. B., Smolyakov, G. A., Gray, A. L., Lester, L. F., Eliseev, P. G. and Osiński, M., “Highly unidirectional InAsInGaAsGaAs quantum-dot ring lasers,” Appl. Phys. Lett. 86(20), 1–3 (2005).
[7] Liang, J. J., Lau, S. T., Leary, M. H. and Ballantyne, J. M., “Unidirectional operation of waveguide diode ring

lasers," Appl. Phys. Lett. 70(10), 1192–1194 (1997).
[8] Cai, X., Yu, S., Chen, Y. and Zhang, Y., "Nonlinearity in Semiconductor Micro-Ring Lasers," Compact Semicond. Lasers 9783527410, 257–296 (2014).
[9] Oku, S., Okayasu, M. and Ikeda, M., "Low-Threshold CW Operation of Square-Shaped Semiconductor Ring Lasers (Orbiter Lasers)," IEEE Photonics Technol. Lett. 3(7), 588–590 (1991).
[10] Liang, D., Kurczveil, G., Fiorentino, M., Srinivasan, S., Fattal, D. A., Huang, Z., Bowers, J. E. and Beausoleil, R. G., "Hybrid III-V-on-Silicon Microring Lasers," MRS Proc. 1538, 363–369 (2013).
[11] Osinski, M., Kalagara, H., Lee, H. and Smolyakov, G. A., "Structure-induced asymmetry between counterpropagating modes and the reciprocity principle in whistle-geometry ring lasers," 70 (2017).
[12] Snyman, L. W. and Okhai, T., "Design and simulation of optical micro-structures in silicon integrated circuitry with Si avalanche-mode light emitters, EXCEL optical ray tracing, and RSOFT optical simulation," 24 January 2019, 47, SPIE-Intl Soc Optical Eng.
[13] Hayenga, W. E., Parto, M., Ren, J., Wu, F. O., Hokmabadi, M. P., Wolff, C., El-Ganainy, R., Mortensen, N. A., Christodoulides, D. N. and Khajavikhan, M., "Direct Generation of Tunable Orbital Angular Momentum Beams in Microring Lasers with Broadband Exceptional Points," ACS Photonics 6(8), 1895–1901 (2019).
[14] Mezosi, G. and Sorel, M., "Semiconductor Micro-Ring Lasers," Compact Semicond. Lasers 9783527410, 231–256 (2014).
[15] Ren, J., Parto, M., Wittek, S., Hokmabadi, M. P., Christodoulides, D. N. and Khajavikhan, M., "Unidirectional Light generation in PT-symmetric Microring Lasers," 2018 Conf. Lasers Electro-Optics, CLEO 2018 - Proc. 26(21), 27153–27160 (2018).
[16] Sacher, W. D., Davenport, M. L., Heck, M. J. R., Mikkelsen, J. C., Poon, J. K. S. and Bowers, J. E., "Unidirectional hybrid silicon ring laser with an intracavity S-bend," Opt. Express 23(20), 26369 (2015).
[17] Ghillino, E., Pasella, P., Staffer, R., Richards, D., Patel, J., Mena, P., Scarmozzino, R., Bardella, P., Virgillito, E., Pilori, D., Carena, A. and Curri, V., "Assessing the impact of design options for an optical switch in network routing impairments," Int. Conf. Transparent Opt. Networks 2019-July, 1–4 (2019).